Three-dimensional estimation of electron density over Japan using the GEONET GPS network combined with SAC-C data and ionosonde measurements

M. Garcia-Fernandez,[1] A. Saito,[2] J. M. Juan,[3] and T. Tsuda[1]

Received 31 January 2005; revised 12 May 2005; accepted 4 August 2005; published 11 November 2005.

[1] The work presented here proposes a local tomographic approach to obtain a three-dimensional description of the ionospheric electron density over Japan. To do this, a combination of GPS and ionosonde data is used in order to take advantage of the strong points of each data type. The GPS data is composed of ground and SAC-C Low Earth Orbiter observations. The ground observations correspond to measurements of 99 receivers (out of about 1000) from the dense Japanese GPS network (GEONET). SAC-C GPS limb sounding observations are processed to obtain vertical profiles of electron density. For this purpose, an improved approach of Abel inversion that considers Vertical Total Electron Content data has been used to overcome the assumption of spherical symmetry. The resulting profiles have been averaged to build a set of background profiles, which are rescaled with the ionospheric NmF2 values sounded by the Japanese network of four ionosondes and used by the tomographic algorithm to provide with vertical description of electron density. For the validation of this tomographic approach, the hourly values of NmF2 given by the four Japanese ionosondes and the vertical profiles of electron density measured by the MU Radar in Shigaraki (during the sounding campaign of November 2002) have been used. This validation with independent data shows relative discrepancies about 25% and, moreover, it shows that the use of the profiles obtained from SAC-C data offers an improvement on the dawn, dusk, and nighttime bottomside and topside estimations of the electron density with respect to the case of using the IRI model.

Citation: Garcia-Fernandez, M., A. Saito, J. M. Juan, and T. Tsuda (2005), Three-dimensional estimation of electron density over Japan using the GEONET GPS network combined with SAC-C data and ionosonde measurements, *J. Geophys. Res.*, *110*, A11304, doi:10.1029/2005JA011037.

1. Introduction

[2] Since the first introduction by *Austen et al.* [1988], the estimation of the ionospheric electron content using tomographic techniques has been the object of numerous studies and improvements as done, for instance, by *Raymund et al.* [1990], *Yeh and Raymund* [1991], or *Fremouw et al.* [1992]. With the advent of Global Positioning System (GPS), the possibilities of ionospheric tomography have been increased, in particular the possibility to perform either global and local four dimensional tomography [*Howe et al.*, 1998]. Nevertheless, the use of ground GPS receivers does not easily allow to solve for the vertical distribution of the ionospheric electron density [*Yeh and Raymund*, 1991]. This is basically due to the geometry of the observations associated to this type of observable, mainly vertical ray paths. This problem can be solved, for instance, by considering a background model of the ionosphere, or by using data complementary to ground GPS observation. In this context it can be used the GPS observations gathered by Low Earth Orbiters (LEO), since their associated observations correspond to horizontal line-of-sights [*Hajj et al.*, 1994; *Howe et al.*, 1998; *Hernández-Pajares et al.*, 1998]. Alternatively, as done by *Garcia-Fernandez et al.* [2003a], the ground GPS solution can be constrained with vertical profiles of electron density from the IRI model [*Bilitza*, 2001] or NeQuick model [*Hoccheger et al.*, 2000] anchored with ionosonde measurements.

[3] This work proposes a local study of ionospheric tomography into the regional zone of Japan (20°N to 50°N of latitude and 120°E to 150°E longitude). In this area it is possible to make use of the dense GPS network (more than 1000 receivers) operated by the Japanese Geographical Survey Institute (GSI), the GPS Earth Observation Network (GEONET) [*Miyazaki et al.*, 1997]. Several works have already shown the high potential of this network to obtain detailed ionospheric information, for instance the

[1]Research Institute for Sustainable Humanosphere, Kyoto University, Kyoto, Japan.
[2]Department of Geophysics, Kyoto University, Kyoto, Japan.
[3]Department of Applied Physics, Universitat Politécnica de Catalunya, Barcelona, Spain.

0148-0227/05/2005JA011037

high-resolution Vertical Total Electron Content (VTEC) maps [*Saito et al.*, 1998].

[4] As mentioned before, an important issue in ionospheric tomography is how is dealt with the vertical resolution. In this case, data from the SAC-C satellite, with nominal orbit of 700 km, is used. However, the problem of using the raw LEO GPS data (as done with global tomography by *Hajj et al.* [1994], *Howe et al.* [1998], or *Hernández-Pajares et al.* [1998]) in a local approach is the high sparsity of this data either in space or time. Therefore it is not possible to fully describe the three-dimensional structure of the electron density. The solution based on the use of background vertical profiles of electron density analogous to works such as *Raymund et al.* [1993] or *Mitchell et al.* [1997] will be adopted here.

[5] Nevertheless, for this work, instead of a model, vertical profiles of ionospheric electron density obtained from SAC-C occultations have been used. These profiles have been computed using the Abel inversion [see, e.g., *Hardy et al.*, 1993; *Hajj and Romans*, 1998; *Schreiner et al.*, 1999] with a modification to include VTEC information to overcome the spherical symmetry assumption [*Hernández-Pajares et al.*, 2000; *Garcia-Fernandez et al.*, 2003b]. To build the background profiles, these profiles have been averaged according to different ionospheric conditions of latitude, season, and local time and afterward rescaled using the measurements provided by the Japanese network of four ionosondes: Okinawa (127.8E 26.3N), Yamagawa (130.6E 31.2N), Kokubunji (139.5E 35.7N), and Wakkanai (141.7E 45.4N).

[6] The paper is structured as follows: Section 2 will describe how the vertical information provided to the tomographic model is computed, section 3 contains the description of the tomographic algorithm, and section 4 includes the validation of the technique using independent data to the model (data from the Japanese ionosondes and the vertical profiles of electron density measured by the MU Radar).

2. Background Vertical Profiles

[7] In a local context the problem of using direct observations from LEO data to obtain vertical information for the tomographic process is its high sparsity. This sparsity is both in space and time, thus making it difficult to obtain occultations for a specific region the 24 hours of the day. With more dense LEO constellations such as COSMIC [*Rocken et al.*, 2000] this issue may be solved, but for this work, an alternative approach is suggested based on providing the model with a set of background profiles, a similar approach used by *Raymund et al.* [1993] or *Mitchell et al.* [1997]. However, in the work proposed here, the vertical information is included to the algorithm in the form of constrains on the cells.

[8] In order to obtain this set of background profiles, the work proposes the use of average profiles of electron density obtained from the SAC-C satellite. The SAC-C LEO has been chosen due to its high orbit (700 km) in front of other LEOs such as CHAMP, with lower initial nominal orbit at 450 km (decreasing due to atmospheric drag), so higher vertical profiles, up to the satellite orbit, can be obtained. The vertical profiles are obtained by means of the Abel inversion algorithm in which the limitations due to spherical symmetry assumption have been overcome. This is done by means of including VTEC information to the inversion process to account for the horizontal gradients of electron density (see *Hernández-Pajares et al.* [2000] and *Garcia-Fernandez et al.* [2003b] for further details). With this approach, it is assumed a separability of the electron density profiles between a shape function (F, which is in fact a vertical descriptor of the variation of electron density) and the VTEC (which accounts for the horizontal variations). Therefore the electron density profiles can be obtained by rescaling the shape function with VTEC at the geographical location:

$$N_e(\lambda, \phi, h) = VTEC(\lambda, \phi) \cdot F(h) \quad (1)$$

where λ, ϕ, and h are longitude, latitude, and height, respectively. N_e is the electron density, VTEC is the Vertical Total Electron Content, and F is the shape function, which is obtained from each occultation.

[9] The main feature of the F function is that it shows less geographical and local time dependency than the electron density profiles (N_e). The variations are basically due to changes in height rather than amplitude, since the electron density variations are partially taken into account by the VTEC information. An example of this characteristic can be seen in Figure 1, where it is shown that although the shape functions correspond to different local times, only differences in height of the profiles and shape of nighttime bottomside are relevant. If N_e profiles would compared instead, besides these differences in height reported for the shape functions, large variations in amplitude would take place as well. Therefore grouping shape functions to obtain average profiles is more consistent than grouping N_e directly.

[10] To obtain the average profiles, the limb sounding data for the SAC-C satellite corresponding to the year 2002 has been processed using the improved Abel algorithm, leading to nearly 29,000 shape functions. Afterward, the average profiles are computed by grouping the individual profiles and averaging them. The sets are built on the following basis:

[11] 1. The first consideration is season. Three sets have been considered: summer (from day of year (doy) 172 to 263), winter (from doy 355 to 79), and equinox (which contain both spring and autumn, that is from doy 80 to 171 and from doy 264 to 354).

[12] 2. The second consideration is local time, namely daytime (from 8 hours local time (LT) to 20 hours LT) and nighttime (from 20 hours LT to 8 hours LT). This coarse distinction is performed due to the fact that seeing the tangent points of the SAC-C occultations in local time (see Figure 2), the latitudes of interest (20 to 50 for Japan) are only covered in two local times, around 10 hours LT and 23 hours LT. This is obviously a limitation to the model since day or night profiles cannot explain the rapid changing of the profiles during dawn and dusk periods. Figure 3 illustrates this problem. The electron density profiles obtained by the MU Radar of Shigaraki since 1999 have been converted to shape function by dividing the profiles by the corresponding VTEC from the Global Ionospheric Maps in IONEX format (see equation (1)). Once obtained, they have been averaged in a hourly basis on the one hand and with the scheme used for the SAC-C profiles (day/time

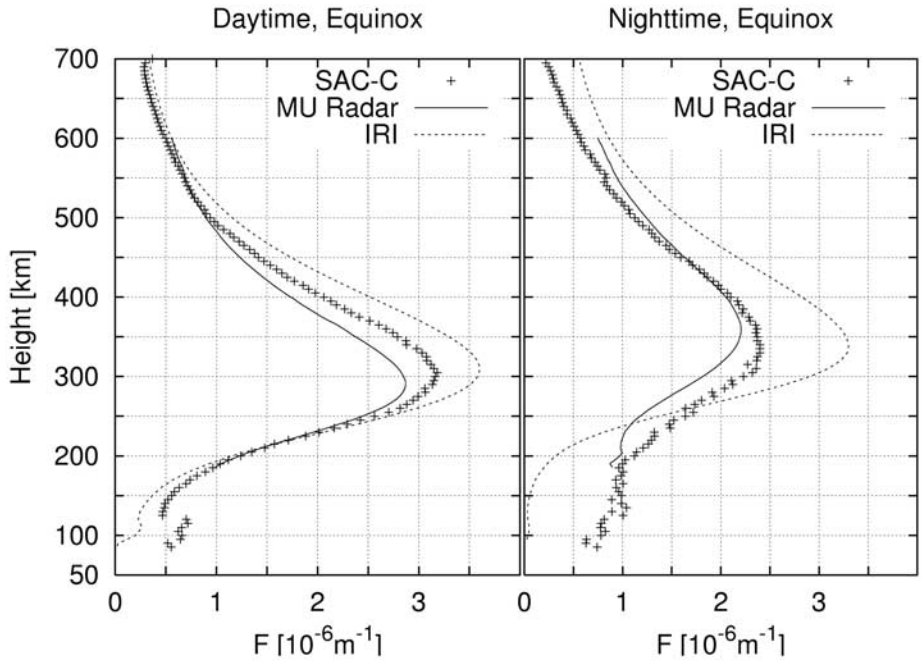

Figure 1. In this figure it is depicted the daytime and nighttime averages of profiles corresponding to (1) The SAC-C satellite corresponding to the latitude band 30°–35° and equinox, (2) the IRI model for the same latitude band and season (the IRI model has been run to compute several profiles and they have been afterward averaged), and (3) the averaged Shigaraki (latitude of 34.85°) MU Radar profiles (gathered during the sounding campaigns from mid-1998 to mid-2003).

division) on the other. Afterward, the shape functions values of each local time profile are compared with the shape function value at the same height of the corresponding day or night average profile (8 hours ∼ 20 hours LT are associated to day profiles and otherwise to night profiles). See upper left panel for a particular case of a dawn profile; it is the 6 hours LT profile, which is associated to a night profile. This is done in order to check to what extent the

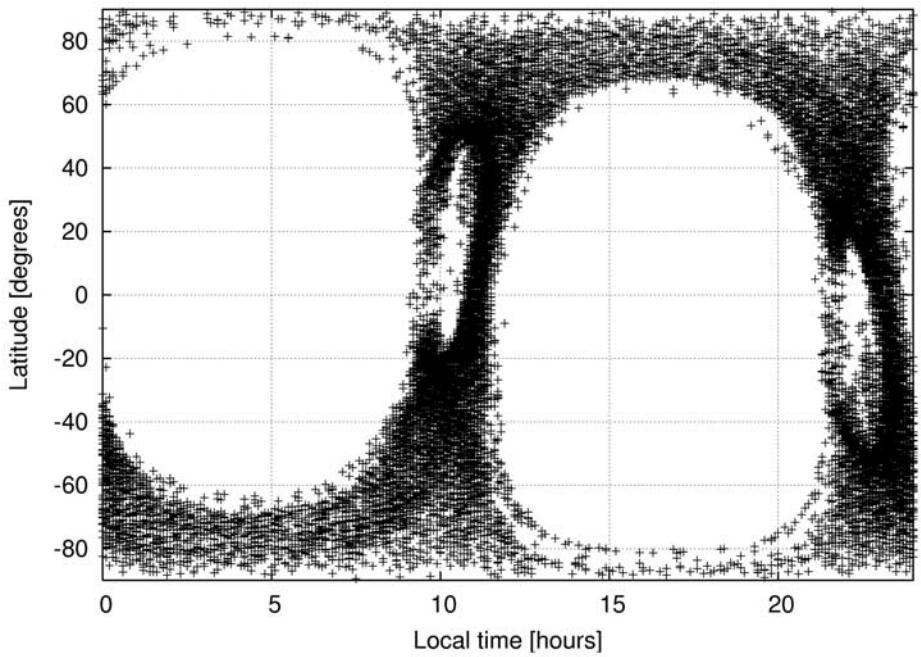

Figure 2. Tangent point of SAC-C in local time. All events of year 2002 are depicted, showing two bands corresponding at daytime (around 10 hours LT) and nighttime (around 23 hours LT).

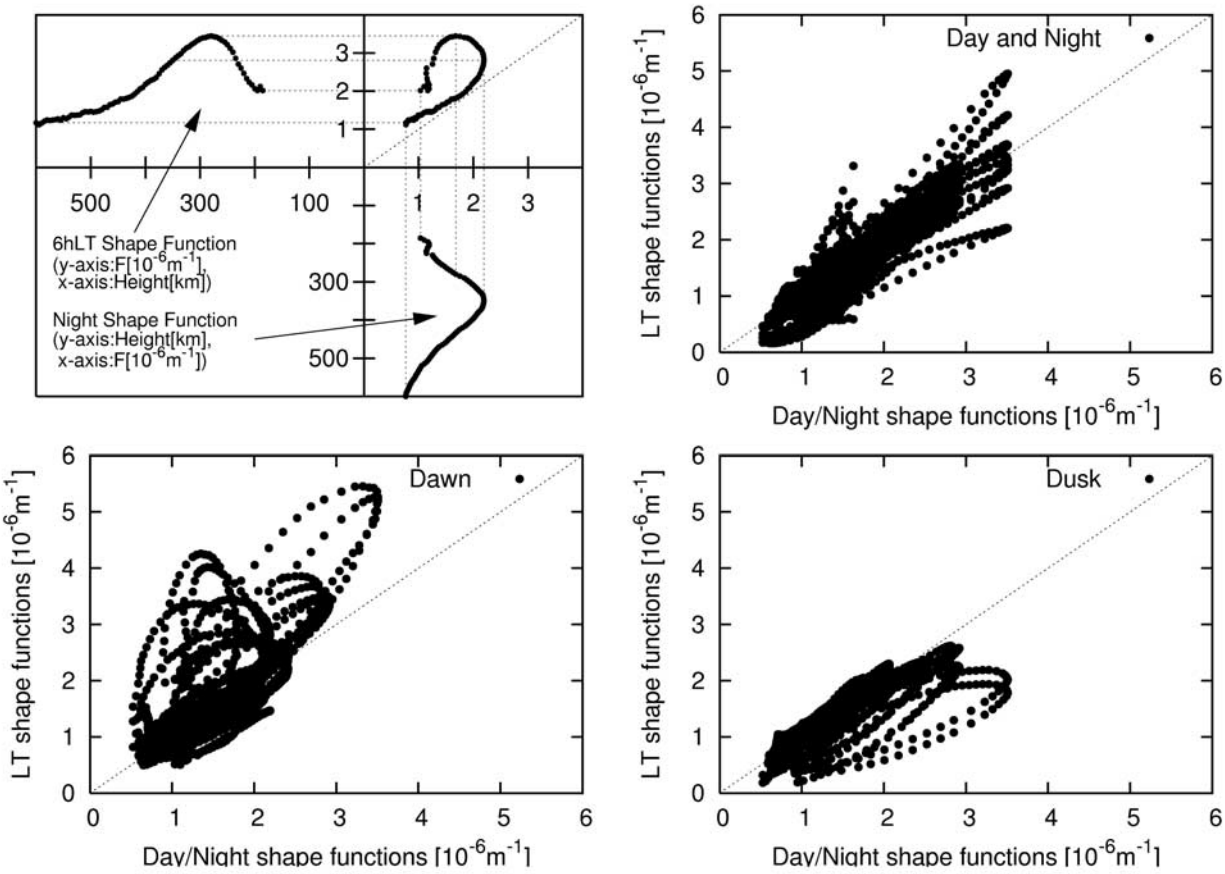

Figure 3. Comparison between the day/night average of profiles and hourly profiles from Shigaraki MU Radar soundings. Upper left panel shows a particular case between the 6 hours LT shape function (F) and the night shape function. Upper right panel shows all local time shape function comparison between the interval 22 hours $\sim$ 4 hours LT and 10 hours $\sim$ 17 hours LT. Lower left panel shows the case for the dawn profiles (5 hours $\sim$ 9 hours LT) and lower right the case for the dusk period (18 hours $\sim$ 21 hours LT).

day/night profiles can explain the dawn and dusk periods. Upper right panel shows the comparison for the profiles with local times in the following intervals: 22 hours LT $\sim$ 4 hours LT (associated to night profiles) and 10 hours LT $\sim$ 17 hours LT (associated to day profiles). With only day or night profiles, there is a good matching (regression line $1.03 \times x + 0.00$, $r^2 = 0.89$). The lower plots depict that this assignation shows less good matching in the dawn and dusk profiles due to the rapid change of the profiles during these periods. This limitation will have implications in the results as it will be seen afterward.

[13] 3. The third consideration is latitude. The profiles have been grouped in intervals of 5° in latitude.

[14] No distinction has been made for the geomagnetic activity because the profiles of this data set do not show large discrepancies, and besides, the number of occurrences of high geomagnetic activity (assumed to be epochs with K_p index larger than 4) for the data set of the SAC-C is not large enough to provide with reliable averaging.

[15] In this work it is proposed the use of real data (in this case from the SAC-C LEO) instead of a model such as the IRI because it is possible to obtain more realistic profiles than a climatologic model as it can be seen in Figure 1 with a particular example of comparison with the averaged profiles obtained from the MU Radar in Shigaraki. This figure shows three averaged profiles for the Shigaraki location in Japan (136.1E 34.85N) according to three different data types: (1) the SAC-C occultations, (2) the IRI model, and (3) the MU Radar soundings. For this latter type, the VTEC from the IONEX maps has been used in order to construct the shape functions (see equation (1)), since the VTEC obtained from the MU Radar profile is underestimated (only N_e values from 180 km to 600 km are obtained). The choice of SAC-C profiles instead of a model such as IRI is supported by the reasonable matching between the LEO and MU Radar average profiles, specially during daytime. The nighttime case, although the MU Radar profile starts from 180 km and taking into account the relative displacement in height between this profile and the SAC-C profile, there is more consistency in the bottomside and their amplitudes when compared with the IRI model.

[16] As mentioned before, to obtain the N_e profile from the shape functions, the VTEC is needed. However, an alternative way to rescale the profiles, and the one actually

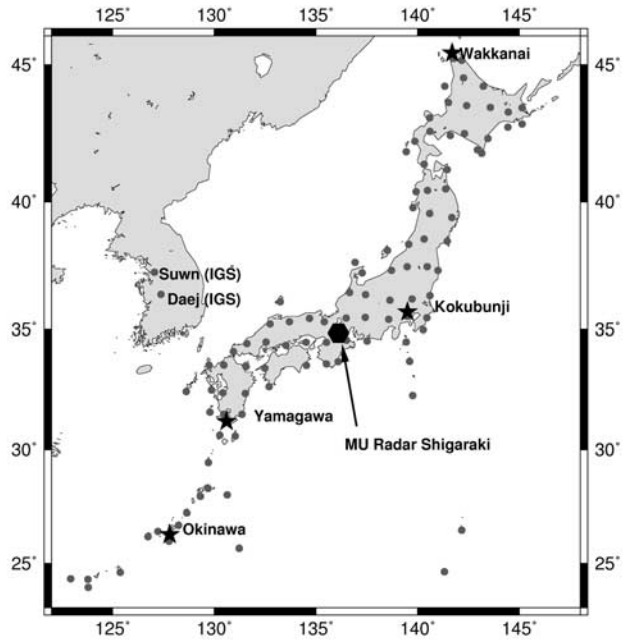

Figure 4. Map depicting the network of GPS receivers (grey circles, 99 GPS receivers from the Japanese GEONET GPS network and two additional Korean receivers from the International GPS Service), four Japanese ionosondes (black stars), and the MU Radar at Shigaraki (black hexagon).

used in this work, consists in using the electron density maximums of the F2 layer (NmF2) measured by ionosondes, so it is possible to take advantage of the high precision NmF2 values measured by the ionosondes during daytime.

[17] The maximums of electron density of the F2 layer (NmF2) are provided by the network of the four Japanese ionosondes (black stars in Figure 4). Moreover, each average profile has associated the corresponding standard deviation for each height. In order not to "freeze" the profiles in the tomographic algorithm and to allow it to take into account the GPS data as well, this standard deviation values have been introduced to the algorithm as a measure of the "noise" for the profiles. The average relative value of the standard deviation with respect to the mean of the profile is of 29% for daytime and 56% for nighttime.

3. Technique

[18] Following the idea of data combination proposed by *Garcia-Fernandez et al.* [2003a], this work combines several data types in order to obtain a three-dimensional description of the ionosphere. The main features of the approach proposed in this paper are as follows:

[19] 1. The use of the subset of 99 out of more than 1000 GPS receivers from the GEONET network (see Figure 4) in order to take advantage of the high density of GPS receivers over the Japanese islands and obtain a more detailed description of the ionosphere in the horizontal dimension.

[20] 2. Instead of using profiles from models such as IRI or NeQuick, vertical profiles obtained from the SAC-C occultation data will be used to construct a set of background profiles.

[21] To check the validity of this background information in a tomographic context using a simple technique, an RMS approach has been chosen to combine both data types.

3.1. Ionospheric Grid

[22] In this work, to obtain the three-dimensional spatial distribution of the electron density, the ionosphere is considered to be a set of volume elements or "voxels," where the electron content in each voxel is assumed to be constant. The proposed approach uses an irregular grid in the horizontal dimension, no voxels are considered above the seas, only above Japanese islands. This is justified by the lack of receivers in the seas that surround Japan (that may lead to a poorly "illuminated" cells) and the objective of obtaining an average horizontal resolution of $0.5^\circ \times 0.5^\circ$ inside Japan taking into account that a reasonable processing time requires to limit the number of unknowns.

[23] Over each center, a column of nine cells has been considered in order to provide with the vertical description of electron density: the centers have been set to 100, 150, 200, 250, 300, 350, 400, 600, and 800 km, with lower and upper boundaries of ionosphere at 60 km and 1000 km, respectively. The border of each cell is determined as the midpoint between each surrounding center.

[24] Once the ionospheric grid has been configured, the longitude of the cells are translated into local time, in order to make the tomographic program to run in a Sun-fixed reference frame and make use of the stationarity of the ionosphere in this reference frame. As the geographical extension of the area of interest is small, owing to the Earth rotation an individual cell can be illuminated only during few hours. For the scope of this work, more sophisticated techniques such as Kalman filtering are not necessary, therefore each epoch is processed independently, so it is unnecessary to establish a process noise for the electron content of the cell.

3.2. Ground GPS Data

[25] As mentioned before, the ground GPS data consists of 99 GPS receivers from the GEONET network plus two IGS receivers in the Korean peninsula (see Figure 4). The receivers from the GEONET network have been selected on the following basis: a horizontal grid of $1^\circ \times 1^\circ$ in longitude and latitude has been used and the nearest receiver to the cell center has been searched.

[26] The GPS observable used in this work is the phase ionospheric combination (L_I), which can be modeled as

$$L_I \equiv L_1 - L_2 \simeq \alpha \cdot \sum_i \sum_j \sum_k N_e(i,j,k) \cdot l(i,j,k) + b_{Rx}^{GPS}, \qquad (2)$$

where L_1 and L_2 are the GPS phase observables for both frequencies, α is a constant of value 1.0506 m of $L_I 10^{17}$ e/m^2, N_e is the electron density in the (i, j, k) cell, l is the length of the ray path in the cell (i, j, k), and b is an offset constituted by the phase ambiguity and the instrumental delays. This offset b is present due to the fact that this work uses the phase observable instead of the code pseudorange in order to minimize the noise of the GPS observations.

[27] The objective of this work consists therefore in solving the inverse problem. That is, given the L_I observations, to solve for the electron densities and offsets. To do this, batches of 3 hours of ground GPS data sampled each 30 s are jointly processed.

[28] Only 99 out of the more than 1000 available GPS receivers of the GEONET network have been used, mainly because this number of receivers provides with enough data to check whether or not the SAC-C profiles are valid enough to provide the tomographic model with vertical information of electron density. A secondary reason is related to a computational one, increasing the number of receivers imply the increase of number of observations and the unknowns associated to the offsets as well as the time process, eventually causing the program not able to cope with either the number of unknowns and observations.

[29] Since with ground GPS data alone one can expect good estimates of VTEC but not vertical information of electron density, vertical profiles obtained from the SAC-C occultations are used, as explained in the previous section, as a background vertical profiles for the model. To estimate the solution for the grid, the algorithm chooses the most appropriate profile for each vertical column of cells according to season, local time, and latitude. The relation between the weights of the vertical profiles and the ones for the ground GPS information is set to 300, which is the average number of rays that illuminate each cell. With this difference in weight, it is intended that the vertical information do not vanish among the large number of GPS observations for each cell.

4. Results

[30] The period of the data set processed in this work runs from 11 November 2002 to 15 November 2002. The averaged profiles from the SAC-C satellite correspond to those of the Japan latitudes (from 20 to 50 degrees in latitude) and the equinox set (a total number of 14 profiles are used, according to the grouping criteria explained above). The k_p index for this period is equal or smaller than 4; therefore no large ionospheric disturbances took place.

[31] For the validation of the method, two types of comparison with real data have been considered, comparison of NmF2 value of ionosondes that have not been taken part into the process and the vertical profiles of electron density corresponding to the MU Radar at Shigaraki (see location at Figure 4).

4.1. Ionosonde Comparison (NmF2 Assessment)

[32] To perform a partial validation of the tomographic estimation, it is given a comparison with the hourly values of NmF2 provided by the four Japanese ionosondes (see Figure 4 for location) that provide with precisions in general better than 4%. It is necessary to distinguish between the ionosondes that were used in the process (constrained ionosondes) and the ones independent to the process that are used in the comparison (test ionosondes). Two different cases are proposed, one with one constrained ionosonde (Kokubunji, center part of Japan) and another one with two constrained ionosondes (Okinawa and Wakkanai, southernmost and northernmost part of Japanese archipelago, respectively). The results are shown in Table 1. During daytime, the agreement is close to a relative discrepancy of 25% or $0.4 \cdot 10^{12}$ e/m^3 in absolute units). During nighttime however the values of electron densities are lower, leading to a lower values in the absolute discrepancies but larger in relative. Moreover, Figure 6 shows the local time dependency of the relative discrepancies. It can be seen that the lowest ones correspond during daytime, with a systematic increasing during dawn. On the contrary they are larger in general during the rest of the periods. The increase in the dawn period corresponds to sudden changes in both the shape of the profiles and the value of the NmF2 (larger than dusk period, see Figures 5 and 6 to check this variability), thus leading to an increase in the discrepancies between the estimation and the reference given by the ionosonde. For the period of study, the number of ionosonde measurements (and therefore for comparison) is 4×120 (hourly soundings).

Table 1. Discrepancies of Estimated NmF2 With Respect to the Values Provided by Ionosondes During the Period Running From November 11 2003 to November 15 2002[a]

	Day		Dawn and Dusk		Night	
	10 ∼ 17 hours LT		5 ∼ 9 hours LT, 18 ∼ 22 hours LT		22 ∼ 4 hours LT	
	Abs.[b]	Rel.[c]	Abs.[b]	Rel.[c]	Abs.[b]	Rel.[c]
Wakkanai	0.35	21.9	0.40	64.0	0.09	38.3
Kokubunji(*)	0.45	22.7	0.37	49.2	0.10	34.6
Yamagawa	0.44	20.6	0.31	37.8	0.20	48.5
Okinawa	0.73	27.7	0.64	41.4	0.46	48.5
Wakkanai(*)	0.07	3.3	0.04	5.0	0.02	6.5
Kokubunji	0.81	35.3	0.73	93.8	0.44	138.3
Yamagawa	0.82	31.3	0.71	78.3	0.37	85.1
Okinawa(*)	0.08	2.2	0.09	6.1	0.08	7.4

[a]The NmF2 measured by the ionosonde has been compared with the NmF2 value of the estimated profile corresponding to the closest center of the ionosonde. Asterisk marks the constrained ionosonde.
[b]Absolute, 10^{12} e/m^3.
[c]Relative, in percentage.

[33] Note the increase discrepancy during nighttime in the Okinawa ionosonde. This is due to the fact that the behavior of the test ionosonde can not be correctly accounted for if the constrained ionosonde does not observe the same behavior. See in Figure 5 that the Okinawa ionosonde, closer to northern Appleton anomaly, measures large enhancements of NmF2 during dusk and night. These enhancements do not take place in the rest of ionosondes. The VTEC estimation (lower panel of Figure 5) follows this enhancement to a certain extent. In fact, the ground GPS data can cope with this variation to a certain degree as seen in Table 1; however, owing to this reason an increase of discrepancy in the Okinawa ionosonde takes place when only Kokubunji is constrained. This effect can be seen as well if the ionosondes of Okinawa and Wakkanai are constrained. In this case the Okinawa ionosonde introduces ionospheric information that does not actually explain the behavior of Kokubunji and Yamagawa, thus leading to a worse estimation. An additional point to mention in Table 1 is the larger discrepancy for the Kokubunji ionosonde when it is constrained (compared with the case of Wakkanai and Okinawa). This is due to the fact that the number of

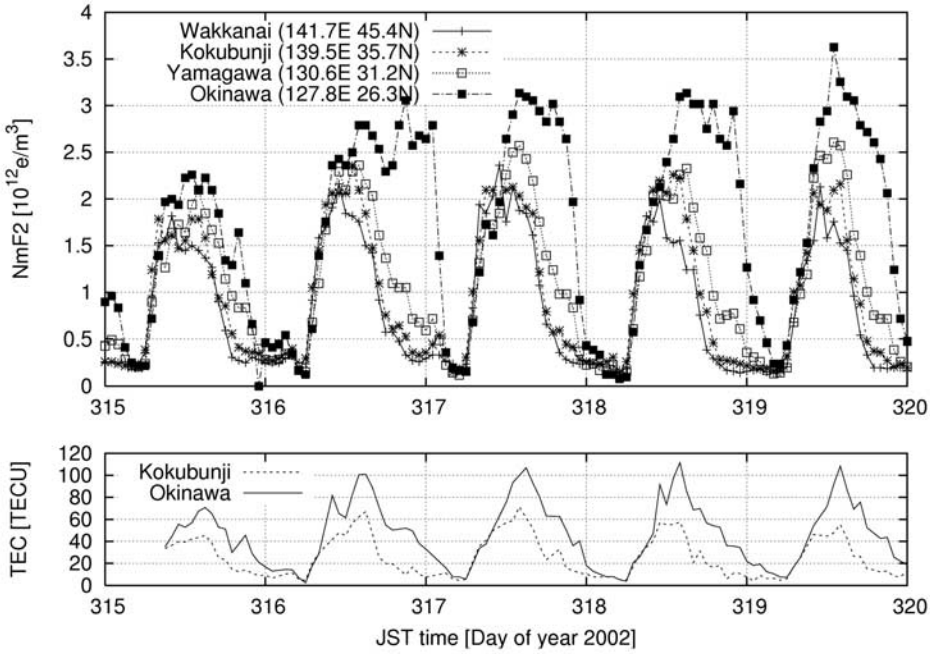

Figure 5. (top) NmF2 measured by the Japanese ionosondes (Wakkanai, Kokubunji, Yamagawa, and Okinawa) during the period of study, from 11 November (day of year 315) to 15 November 2002 (day of year 319). (bottom) VTEC measured with ground GPS data corresponding to the locations of Kokubunji and Okinawa during the period of study. Timescale for both panels is Japanese Standard Time (JST, Japan local time), expressed in day of year.

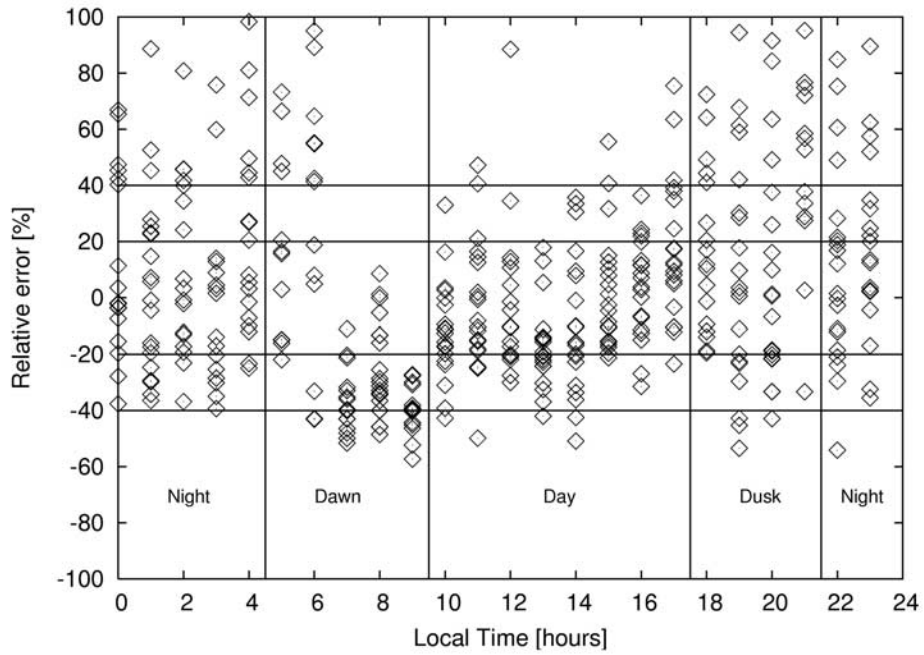

Figure 6. Evolution of the relative discrepancies with the comparison of NmF2 measured by the ionosonde with the local time. X-axis is the local time in hours and y-axis is the relative discrepancy of the tomographic estimation of the NmF2 with respect to the reference given by the ionosonde. The estimation is performed constraining the ionosonde of Kokubunji.

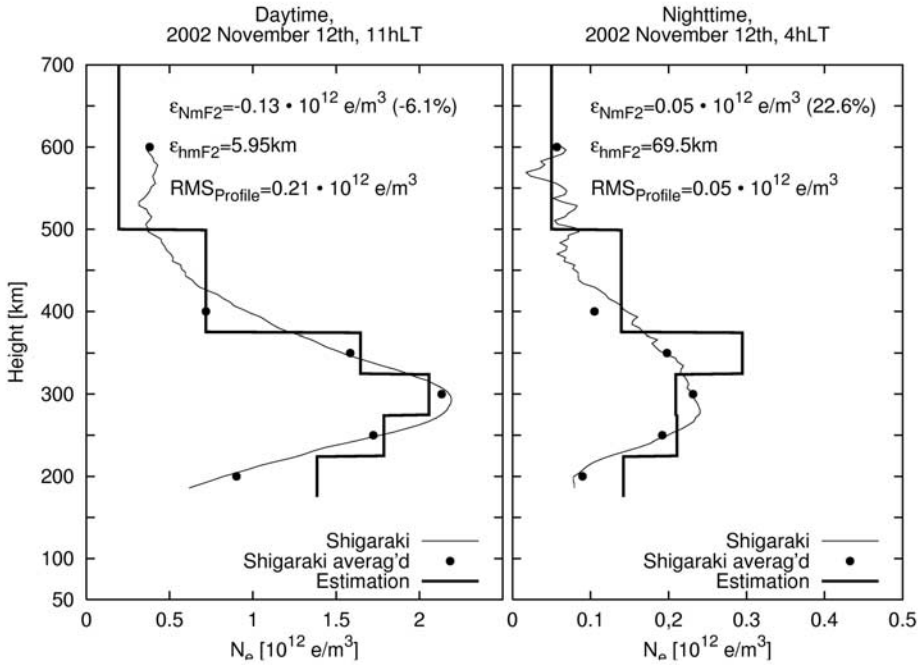

Figure 7. Two particular examples of performance when comparing with N_e profiles measured by the MU Radar of Shigaraki. It is given examples for Daytime and Nighttime (please note the different scales in the x-axis between both cases).

receivers that surround the Kokubunji ionosonde is larger, thus diminishing the relative weight of this ionosonde information.

4.2. MU Radar Comparison (Shape Assessment)

[34] For this comparison, all four ionosondes have been used as a constraint ionosonde to avoid the problem mentioned in the last section. As a validation, the vertical profiles of electron density provided by the MU Radar at Shigaraki (136°6′E34°51′N) gathered during the days of the estimation have been used, since these measurements are independent to the tomographic model. Since the MU Radar provides only with relative measurements of electron density, a calibration of the profiles using the data from the ionosonde of Kokubunji has to be carried out.

[35] The radar profile (reference), which starts around 200 km and ends around 600 km, is averaged according to the distribution in height of the ionospheric grid. Afterward, each point of the profile is compared with the corresponding tomographic estimate, so the profile discrepancy (profile RMS) can be obtained. Owing to the height limitation of the radar, there are only six of the total nine vertical points. Figure 7 shows two particular examples of performance. While the daytime profile shows good agreement either in NmF2 and hmF2, nighttime profile shows a large discrepancy in hmF2.

[36] Table 2 summarizes the results for comparison with the radar soundings. It is shown that the discrepancies in NmF2 for the day, dawn and dusk, and night periods are similar to the previous comparison with ionosonde. Moreover, it is given the comparison with the whole profile in absolute values. Regarding the discrepancies in the hmF2, the comparisons show that the discrepancy is larger during nighttime, dawn, and dusk. This is due to two reasons; the first one is that while during daytime the hmF2 is clearly defined, the nighttime profiles are less sharp and thus it is more difficult to distinguish where the maximum is placed. Moreover, the discrepancies are also due to the background profiles constructed from SAC-C. Looking at the nighttime profile of Figure 1 and the nighttime example of Figure 7, it can be seen that the hmF2 in both cases are similar (close to 350 km), but the actual case measured by the Shigaraki radar for this time points the hmF2 value to 280 km approximately. In the case of the discrepancy corresponding to dawn and dusk periods, the reason is due to the rapid changing of shape function during these periods (note that only nighttime or daytime shape functions are considered, as pointed out in previous sections). Regarding the NmF2 and profile RMS, the discrepancies are consistent with the values obtained in the ionosonde comparison.

[37] To give a more general impression of the results, Figure 8 shows the correlation between the N_e estimated by the tomographic approach and the average value of N_e corresponding to the profiles measured by the MU Radar. The correlation coefficient ($r^2 = 0.73$) of the regression line indicates a good consistency between the reference and the estimation.

[38] Moreover, the statistics shown in Table 2 show an additional comparison with respect to the case of using IRI vertical profiles anchored with ionosonde (instead of SAC-C profiles). During daytime, the shape of the rescaled profiles with NmF2 of IRI and SAC-C are almost similar, which explains that the results are similar during this period with both types of profiles or even slightly better for the IRI

Table 2. Discrepancies of Estimated Profile With Respect to the Profiles From the MU Radar at Shigaraki[a]

	Day		Dawn and Dusk		Night	
	10 ∼ 17 hours LT		5 ∼ 9 hours LT, 18 ∼ 22 hours LT		22 ∼ 4 hours LT	
	Abs.[b]	Rel.[c]	Abs.[b]	Rel.[c]	Abs.[b]	Rel.[c]
NmF2	0.28	14.35	0.40	42.65	0.12	36.02
hmF2	37.7	-	62.7	-	57.4	-
Bottomside Profile	0.42	-	0.43	-	0.16	-
Topside Profile	0.31	-	0.23	-	0.14	-
Bottomside Profile (IRI)	0.34	-	0.52	-	0.21	-
Topside Profile (IRI)	0.35	-	0.38	-	0.28	-

[a]It is given as well the discrepancies in NmF2 and hmF2 provided by the Radar. Number of comparisons is the same than ionosonde measurements (hourly measurements), therefore a total number of 120 comparisons are made. However, in the profile RMS comparison, the number of points is 6 times greater (because of the common 6 vertical cells compared).
[b]Absolute, 10^{12} e/m^3 for NmF2 and $RMS_{profile}$ and km for hmF2.
[c]Relative, in percentage.

case. Note, however, that an improvement takes place during nighttime periods, when the shape functions show larger discrepancy, even when the profiles are rescaled with the same ionosonde values. This result is expected if one looks at the differences in the profiles shown in Figure 1.

5. Conclusions

[39] This work proposes a tomographic approach applied to the Japanese GEONET network, in which data from SAC-C limb soundings and ionospheric soundings of the Japanese networks have been used to provide with the vertical information needed to obtain a three-dimensional description of the ionospheric electron content.

[40] The validation of the proposed approach with either ionosonde data and vertical profiles obtained from the MU Radar at Shigaraki are consistent, showing relative discrepancies of 25% during daytime and less than 40% during nighttime and slightly larger than 40% during dawn and dusk. These discrepancies are similar to other profiling techniques such as Abel inversion, with discrepancies comprised between 20% and 40% in comparison of NmF2 of ionosonde).

[41] These results show that the vertical information used in this work (SAC-C shape functions rescaled with ionosonde soundings) is a viable way to provide to tomographic models with vertical information of electron density. Moreover, the use of this type of information offers an improvement over the use of climatological models such as IRI. This is true specially for the dawn, dusk, and nighttime topside and bottomside comparisons. Further improvement is expected in the dawn and dusk periods when shape functions with more detailed local time evolution are available. In particular, future constellation such as COSMIC may greatly help in overcoming this issue as well as to provide new features, such as the possibility to construct specialized set of basis functions for specific regions of the globe or to help in monitoring particular events such as ionospheric storms.

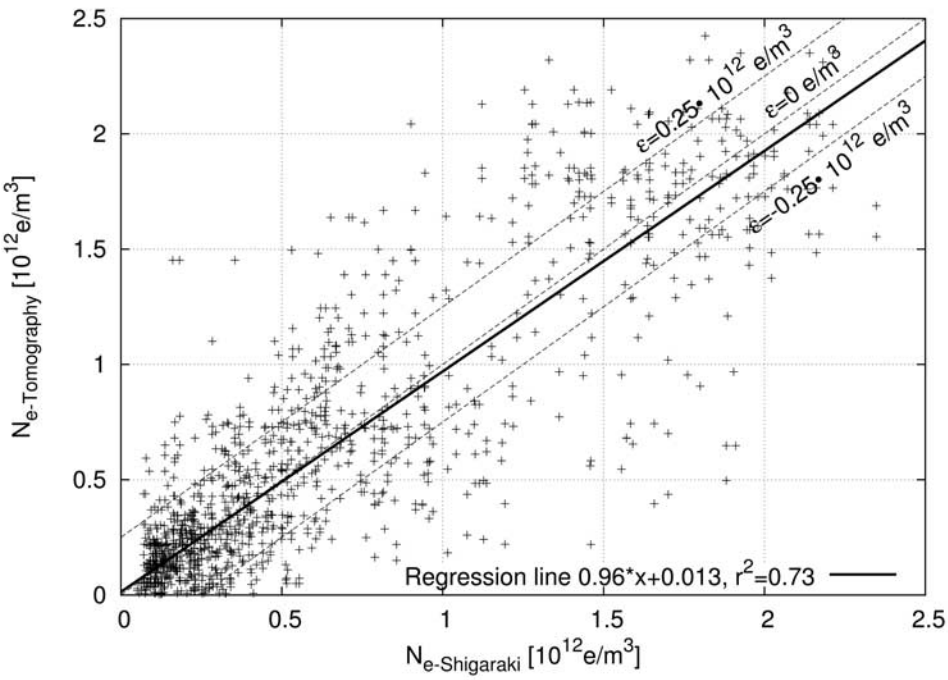

Figure 8. One to one comparison between the electron density values of all heights provided by the MU Radar at Shigaraki and the tomographic estimation. The data set corresponds to the period 11 November 2002 to 15 November 2002. It is also displayed the set of lines showing the absolute errors of 0 e/m^3, $0.25 \cdot 10^{12}$ e/m^3 and $-0.25 \cdot 10^{12}$ e/m^3. The linear regression is also given as well as the regression coefficient ($r^2 = 0.73$).

[42] **Acknowledgments.** Dr. Otsuka (Nagoya University, Japan) and Dr. Kawamura (National Institute of Communications and Information, NICT, Japan) are acknowledged for the data and valuable discussion on MU Radar measurements. The Japanese Geographical Survey Institute provided for the GEONET GPS data. The NICT is acknowledged for the vertical sounding parameters for the Japanese Ionosonde data. SAC-C data has been obtained from the GENESIS JPL ftp server. This research has been fully supported by the Kyoto University Active Geosphere Investigations for the 21st Century COE (KAGI21), which was approved by the Ministry of Education, Culture, Sports, Science, and Technology (MEXT) of Japan.

[43] Arthur Richmond thanks Cathryn Mitchell and another reviewer for their assistance in evaluating this paper.

References

Austen, J. R., S. J. Franke, and C. Liu (1988), Ionospheric imaging using computerized tomography, *Radio Sci.*, *23*, 299–307.

Bilitza, D. (2001), IRI 2000, *Radio Sci.*, *36*, 261–276.

Fremouw, E. J., J. A. Secan, and B. M. Howe (1992), Application of stochastic inverse theory to ionospheric tomography, *Radio Sci.*, *17*, 721–732.

Garcia-Fernandez, M., M. Hernandez-Pajares, J. M. Juan, J. Sanz, R. Orús, P. Coisson, B. Nava, and S. M. Radicella (2003a), Combining ionosonde with ground GPS data for electron density estimation, *J. Atmos. Sol. Terr. Phys.*, *65*(6), 683–691.

Garcia-Fernandez, M., M. Hernandez-Pajares, J. M. Juan, and J. Sanz (2003b), Improvement of ionospheric electron density estimation with the GPSMET occultations using Abel inversion and VTEC information, *J. Geophys. Res.*, *108*(A9), 1338, doi:10.1029/2003JA009952.

Hajj, G. A., and L. J. Romans (1998), Ionosphere electron density profiles obtained with the Global Positioning System: Results from the GPS/MET experiment, *Radio Sci.*, *33*, 175–190.

Hajj, G. A., R. Ibañez-Meier, E. R. Kursinski, and L. J. Romans (1994), Imaging the ionosphere with the Global Positioning System, *Imaging Syst. Technol.*, *5*, 174–184.

Hardy, K. R., G. A. Hajj, E. R. Kursinski, and R. Ibanez-Meier (1993), Accuracies of atmospheric profiles obtained from GPS occultations, paper presented at ION GPS-93 Conference, Inst. of Nav., Fairfax, Va.

Hernández-Pajares, M., J. M. Juan, and J. Sanz (1998), Global observation of the ionospheric electronic response to solar events using ground and LEO GPS data, *J. Geophys. Res.*, *103*, 20,789–20,796.

Hernández-Pajares, M., J. M. Juan, and J. Sanz (2000), Improving the Abel inversion by adding ground GPS data to LEO radio occultations in ionospheric sounding, *Geophys. Res. Lett.*, *27*, 2473–2476.

Hochegger, G., B. Nava, S. M. Radicella, and R. Leitinger (2000), A family of ionospheric models for different uses, *Phys. Chem. Earth*, *25*, 307–310.

Howe, B., K. Runciman, and J. Secan (1998), Tomography of the ionosphere: Four-dimensional simulations, *Radio Sci.*, *33*, 109–128.

Mitchell, C. N., L. Kersley, J. A. T. Heathon, and S. E. Pryse (1997), Determination of the vertical electron-density profile in ionospheric tomography: Experimental results, *Ann. Geophys.*, *15*, 747–752.

Miyazaki, S., T. Saito, M. Sasaki, Y. Hatanaka, and Y. Iimura (1997), Expansion of GSI's nationwide GPS array, *Bull. Geogr. Surv. Inst.*, *43*, 23–34.

Raymund, T., J. Austen, S. Franke, C. Liu, J. Klobuchar, and J. Stalker (1990), Application of computerized tomography to the investigation of ionospheric structures, *Radio Sci.*, *25*, 771–789.

Raymund, T. D., S. E. Pryse, L. Kersley, and J. A. T. Heaton (1993), Tomographic reconstruction of the ionospheric electron density with EISCAT verification, *Radio Sci.*, *28*, 811–817.

Rocken, C., Y. Kuo, W. S. Schreiner, D. Hunt, S. Sokolovskiy, and C. McCormick (2000), COSMIC system description, *Terr. Atmos. Ocean. Sci.*, *11*, 21–52.

Saito, A., S. Fukao, and S. Miyazaki (1998), High resolution mapping of TEC perturbations with the GSI GPS network over Japan, *Geophys. Res. Lett.*, *25*, 3079–3082.

Schreiner, W. S., S. V. Sokolovskiy, C. Rocken, and D. C. Hunt (1999), Analysis and validation of GPS/MET radio occultation data in the ionosphere, *Radio Sci.*, *34*, 949–966.

Yeh, K. C., and T. D. Raymund (1991), Limitations of ionospheric imaging by tomography, *Radio Sci.*, *26*, 1361–1380.

M. Garcia-Fernandez and T. Tsuda, Research Institute for Sustainable Humanosphere, Kyoto University, Kyoto-fu Uji-shi, Gokasho, 611-0011, Japan. (mgarcia@rish.kyoto-u.ac.jp; tsuda@rish.kyoto-u.ac.jp)

J. M. Juan, Department of Applied Physics, Universitat Politécnica de Catalunya, Jordi Girona, 1-3, modul B4-B5, Campus Nord. 08034 Barcelona, Spain. (miguel@fa.upc.es)

A. Saito, Department of Geophysics, Kyoto University, Kyoto, 606-8502, Japan. (saitoua@kugi.kyoto-u.ac.jp)